Check for updates

Impact of type and position of abutment connection on microstrain distribution: an *in vitro* study

Jekita Siripru[1], Usanee Puengpaiboon[2], Chamaiporn Sukjamsri[3], Basel Mahardawi[4], Napapa Aimjirakul[1]*

[1]Department of Conservative Dentistry and Prosthodontics, Srinakharinwirot University, Bangkok, Thailand
[2]Department of General Dentistry, Srinakharinwirot University, Bangkok, Thailand
[3]Department of Biomedical Engineering, Srinakharinwirot University, Nakhon Nayok, Thailand
[4]Department of Oral and Maxillofacial Surgery, Faculty of Dentistry, Chulalongkorn University, Bangkok, Thailand

ORCID
Jekita Siripru
https://orcid.org/0009-0009-4701-1923

Usanee Puengpaiboon
https://orcid.org/0009-0008-3724-5403

Chamaiporn Sukjamsri
https://orcid.org/0000-0002-1976-9544

Basel Mahardawi
https://orcid.org/0000-0001-5113-535X

Napapa Aimjirakul
https://orcid.org/0000-0002-0878-2882

Corresponding author
Napapa Aimjirakul
Department of Conservative
Dentistry and Prosthodontics,
Srinakharinwirot University,
114 Soi Sukhumvit 23, Khlong Toei
Nuea, Watthana, Bangkok 10110,
Thailand
Tel +6626495212
E-mail napapa@g.swu.ac.th

PURPOSE. The aim of this study was to investigate microstrains around two non-parallel implant-supported prostheses and different abutment connections and positions under vertical static load using strain gauges. **MATERIALS AND METHODS.** 4 models simulating the mandibular unilateral free-end were fabricated. 8 implants (4.0 × 10 mm and 5.0 × 10 mm) were inserted in the second premolar, perpendicular to the occlusal plane, and the second molar, tilted at 15°. Four groups were analyzed: engaging and angled abutments (control group), both non-engaging abutments, both screw-and cement-retained prosthesis (SCRP) abutments, and engaging and non-engaging abutments. Strain gauges were placed buccally, lingually, mesially, and distally adjacent to each implant. The restoration was cement-retained in the control group and screw and cement-retained in the rest. Zirconia bridges were fixed on the abutment with NX3, and a 300 N vertical static load was applied. Microstrains were recorded and analyzed. **RESULTS.** Both non-engaging abutments showed the highest compressive microstrains (-52.975), followed by engaging, angled abutment (-25.239). SCRP-SCRP abutments had the lowest compressive microstrains (-14.505), while the engaging, non-engaging abutments showed tensile microstrains (0.418). Microstrains in SCRP-SCRP and engaging, non-engaging groups were significantly lower than in the control group (α = .05). Premolar areas showed compressive microstrains (-47.06), while molar sites had tensile microstrains (+0.91), with microstrains in premolars being significantly higher than in molar area (α = .05). **CONCLUSION.** The types of abutment connections and positions may have a potential effect on microstrains at the implant-bone interface. SCRP-SCRP abutments could be an alternative to use in non-parallel implant-supported prostheses when two implants make an angle of no more than 20 degrees. [J Adv Prosthodont 2024;16:290-301]

INTRODUCTION

Implant-supported bridges have become a standard treatment option for partially or fully edentulous patients, offering high treatment success and patient satisfaction.[1-4] Factors such as bone quality, stress distribution, abutment type, implant dimensions, and positioning influence the longevity of these bridges.[5]

The implant-abutment interface (IAI) plays a pivotal role in determining clinical success. Elevated stress on restoration and implant components can lead to complications like screw loosening, abutment fracture, and implant failure. Factors such as implant connection geometry (external indexed, internal indexed, or cone connection), abutment type (engaging vs. non-engaging), implant materials, positioning, and masticatory forces contribute to stress patterns in the implant-prosthesis-bone complex.[6]

In the traditional method, freehand implant placement is still done. In the posterior region, the deviations between planned and actually achieved position with freehand implant placement showed the mean values and standard deviations as follows: angle $8.7 \pm 4.8°$, 3D deviation at the implant shoulder 1.62 ± 0.87 mm, mesiodistal deviation 0.87 ± 0.75 mm, buccolingual deviation 0.70 ± 0.66 mm, and apicocoronal deviation 0.95 ± 0.61 mm.[7] Freehand implant placement exhibits a higher level of deviation between planned and actually achieved implant position. Moreover, bone anatomy in some areas may be limited in implant angulation, such as maxillary sinus, lingual concavity in the posterior mandible and inferior alveolar canal (IAC). Following dental extraction, bone resorption can occasionally limit the quantity of suitable implants and make it difficult to place the implant in the best possible location. Using a pontic or cantilever (mesial or distal) as an alternative is suggested in this situation to avoid surgical procedures that increase treatment time, cost, and surgical morbidity.[8]

Savignano *et al*.[6] reported that the stress distribution with implants and restorative components can be affected by abutment design (engaging and non-engaging) and location. Engaging abutments are designed to lock into the implant interface's unique anti-rotation feature (hex, star, etc.). With a single unit screw-retained restoration, the engaging abutment is used. This measure will lock the individual crown into the correct orientation (anti-rotation). The non-engaging abutment does not have this anti-rotational feature. Rather, the design does not quite interact or lock the same way between the abutment and implant. This is optional for more than two non-parallel implants. A screw and cement-retained abutment (SCRP) is a specially designed stock abutment with a unique type of connection. In one abutment, there are both engaged and non-engaged components. It has a short-engaged section at the upper half that allows for abutment relocation, as well as a non-engaged section at the lower half. This is feasible due to the SCRP abutment's unique structural design, which includes gaps to compensate the undercuts generated by the nonparallel implant connection.[9]

An implant-supported bridge is more challenging to produce because the impression must be much more precise to connect two or more implants into a single prosthesis. Therefore, the angulation of implants has become more important so that implants are never 100% parallel; passive fit is more difficult to achieve, and more technical precision is required.[1] Nowadays, there are no manufacturer guidelines for selecting the position of an engaging or non-engaging abutment to be connected to the two non-parallel implant-supported bridge. Due to a lack of direct relevant scientific data, this practice is based on anecdotal evidence and the clinical experience of educators and clinicians.[10]

Strain gauge analysis has been widely used to analyze the microstrain distribution of dental implants surrounding bone. Strain gauges are used to evaluate the deformation of force subjected to an implant component.[10]

This *in vitro* study aims to analyze microstrains around two non-parallel implant-supported bridges and investigate the effects of abutment connections and positions using strain gauges. By understanding the impact of these factors on stress distribution, we can optimize treatment strategies for improved clinical outcomes and long-term success. The null hypothesis was that the type and position of the abutment connection have no effect on microstrain at the implant-bone interface around two non-parallel im-

plant-supported prostheses in the posterior region.

MATERIALS AND METHODS

The sample size for this study was determined by Dogus et al.[10] and has been used as a reference in the calculation of sample size for similar studies. A power analysis was performed with a G*Power 3.1.9.4 program. The effect size was 0.7293805 at 95% power; therefore, the minimum sample size for the study was 40. As a result, 10 were used for each group.

Four models for four groups simulating the mandibular unilateral free end were fabricated. Eight implants (4.0 × 10 mm and 5.0 × 10 mm) were inserted in positions representing the second premolar (45) perpendicular to the occlusal plane and the second molar (47) tilted at 15°. Various abutment combinations were used (Table 1, Fig. 1). Strain gauges and static axial loads by universal testing machines were used to measure microstrain around the implant-bone interface. All recordings were repeated 9 times (a total of 10 times for each group).

The lower arch STL file was designed for Kennedy Class II unilateral distal extension of the edentulous area. Resin models were printed using a 3D printer (Metric V3, Formlabs, Somerville, MA, USA), which had a Young's modulus of 2.2 GPa, approximating estimates for trabecular bone (2.2 GPa). Groups 1 – 4 were prepared at 34 – 37 for the fabrication of a monolithic zirconia crown. The models were CT scanned (Whitefox, A company of ACTEON Group, Italy) and model scans were performed using a 3Shape D900L scanner (3Shape A/S, Copenhagen, Denmark). The DICOM and STL files of the model were imported into implant planning software (Fig. 2). The bone-level internally indexed dental implant at position 45 (4.0 × 10 mm, ISIII, Neobiotech, Seoul, Korea) was aligned perpendicular to the occlusal plane, while the implant at position 47 (5.0 × 10 mm, ISIII, Neobiotech, Seoul, Korea) was 15 degrees from the long axis. A static surgical guide was designed, printed, and used for drilling and placing dummy implants according to the Neobiotech protocol.

Stock abutments were connected to the implants

Table 1. Experimental group

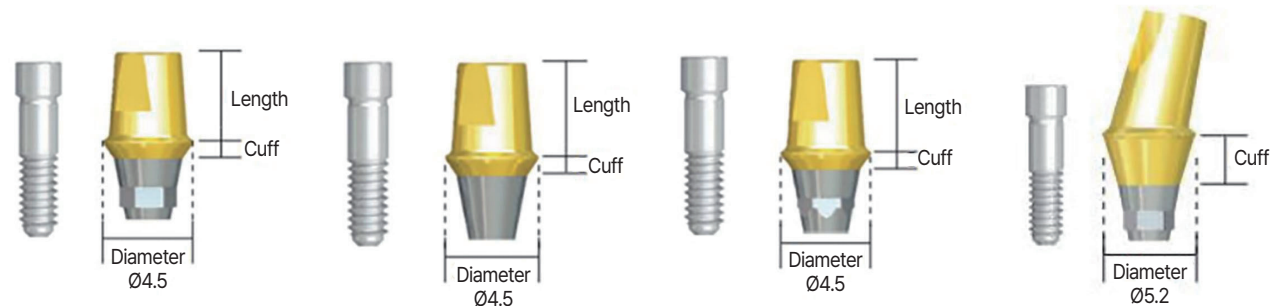| Group (Model no.)	Area 45 Implant (D 4.0 mm L 10 mm) Abutment (D 4.5 H 5.5 GH 1 mm)	Area 47 Implant (D 5.0 mm L 10 mm) Abutment (D 5.2 H 5.5 GH 1 mm) Except group 1, which uses angled abutment 15º (D 5.2 H 7 GH 2 mm)
1	Engaging	Engaging (Angled abutment)
2	Non-engaging	Non-engaging
3	SCRP	SCRP
4	Engaging	Non-engaging

Fig. 1. Engaging, non-engaging, SCRP-type IS cemented abutment and IS angled abutment (Neobiotech, Seoul, Korea).
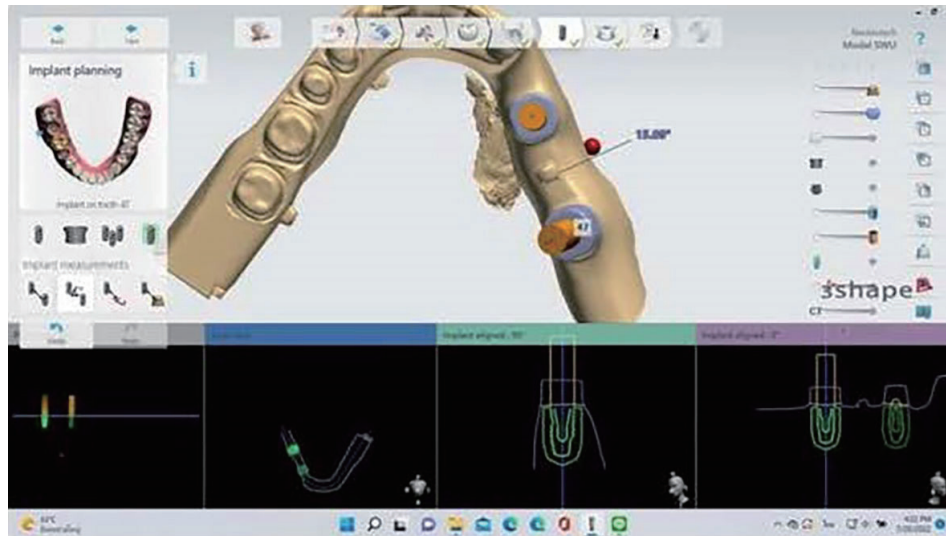
Fig. 2. Dicom and STL files of the model were imported to implant planning software (Implant Studio, 3Shape).

in each model, following groups' designs (Table 1). Torque of 30 Ncm was applied to each abutment twice, following recommendations of the manufacturer (Fig. 3). All abutment screws were tightened before microstrain measurements.

Polytetrafluoroethylene tape (Teflon) was filled at abutment screw access. Prepared zirconia crown on teeth no. 34-37, 4-units zirconia bridge on teeth no. 44 – 47, and both stock abutments in groups 2 – 4 were scanned to design crowns and an implant supported 4-unit bridge with open screw access (Screw and cement-retained restoration). In group 1, they were scanned to design crowns and implant supported 4-unit prosthesis without a screw access (Cement-retained restoration) by the model scanner and Dental System (3shape, Netherland). The monolithic zirconia crown and bridge (Cercon HT, Dentsply Sirona, Bensheim, Germany) were milled as designed by Sainamtip Dental Laboratory (Samut Prakan, Thailand) and a periapical film was taken for verification of the complete seating of the implant-abutment connection in all models. All models received crowns on teeth from the left second molar (tooth 37) until the left first premolar (tooth 34), and a bridge connecting the right second premolar (tooth 44) to the second molar (tooth 47).

A marker line was made to fix the strain gauge on the surrounding bone (i.e., model material in this case), which was 2 mm thick. The 2-mm thick, 360-degree circle of bone was divided into four sections by
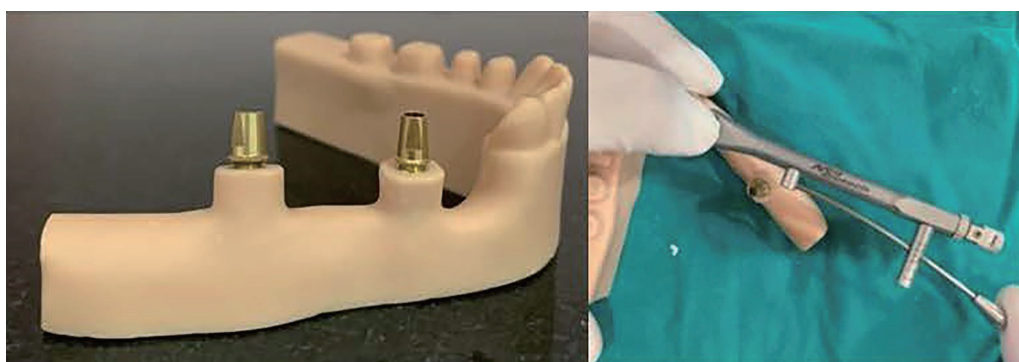

Fig. 3. Stock abutments were connected to any implants and torqued to 30 Ncm (Neobiotech).

making a 90-degree angle. The strain gauge was stabilized in a way that the middle of the gauge is fixed to the marker line and the upper part is attached to the margin of bone (Fig. 4).

Thirty-two strain gauges (KFGS-03-120-C1, Strain Gages, Kyowa Electronic Instruments, Tokyo, Japan) were used in the four models. Eight strain gauges in each model (4 per one implant site) were fixed to the margin of the bone with a cyanoacrylate-based cement (Strain Gage Cement CC-33A, Kyowa Electronic Instruments, Tokyo, Japan) to the mesial, distal, buccal, and lingual regions at the implant-abutment interface area of each 3D-printed model.

Following the manufacturer's instructions, the restoration in all groups was particle-abraded on the intaglio surfaces of the zirconia crowns and zirconia bridges with 50-μm silica particles coated with Al_2O_3 (sandblast) for 10 seconds at a pressure of 2 bar and distance of 10 mm. Then, a silane primer (Kerr, Orange, CA, USA) was applied to the intaglio surface of zirconia crowns and zirconia bridges for 60 seconds and luted after air drying. Finally, zirconia crowns were chemically bonded to the abutments (34 – 37) with resin cement (Kerr, Orange, CA, USA) and the excess cement was carefully removed from the margin. All surfaced were light cured for 20 seconds each. In all groups, an Optibond Solo Plus (Kerr, Orange, CA, USA) was applied to the abutment implants for 15 seconds using a light brushing motion and the adhesive was air-thinned for 3 seconds and then light cured for 20 seconds. Zirconia bridges were chemically bonded to the abutment implants (45,47) with

resin cement (Kerr, Orange, CA, USA) and the excess cement was carefully removed from the margin. All surfaces were light cured for 20 seconds each. Groups 2 – 4 were torqued to 30 Ncm and the access screw hole was covered with composite resin to enhance the restoration's aesthetic and function (Fig. 5).

Strain gauges (KFGS-03-120-C1, Strain Gages, Kyowa Electronic Instruments, Tokyo, Japan) were connected to a data acquisition system (EDX-10 Series, Compact recording system, Kyowa Electronic Instruments, Tokyo, Japan), which delivered the signal to a reading board (EDX-10 Series, Compact recording system, Kyowa Electronic Instruments, Tokyo, Japan) on a desktop computer (Notebook). The strain gauge outputs were evaluated using a data acquisition software (DCS-100A version 04.78, Kyowa Electronic Instruments, Tokyo, Japan). A channel on the data acquisition board were assigned to each strain gauge. All strain gauge values were set to 0 before to connection.

A static axial load (compressive load) of 300 N simulated masticatory force[11-13] was applied at a crosshead speed of 0.05 mm/sec for 15 seconds[14] using the universal testing machine (EZ test, Shimadzu, Tokyo, Japan). A bilateral loading was applied on the first premolar, second premolar, first molar and second molar on each side with a wide strainless-steel plate (Fig. 6). Each loading condition was repeated 9 times. Before each loading, we set all strain gauges to zero. Each strain gauge collected data for strain values. Each strain gauge was used to determine the strain and record the data.
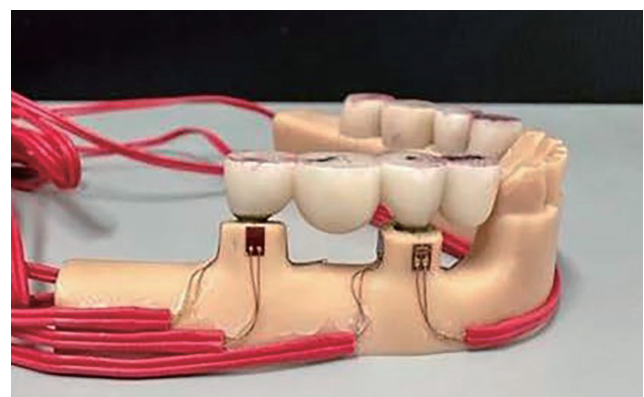

Fig. 4. Location of strain gauges on the model.

Fig. 5. The model after the cementation of crowns and bridges.

Fig. 6. 3D printing model and wide stainless-steel plate.

The analysis of the results of this study was conducted using the statistical software SPSS version 27.0 (SPSS, Inc., Chicago, IL, USA). The normal distribution of data in each sample corner was tested with the skewness/std.error ratio test[15] with the Z test statistics. The sphericity prerequisite of the repeated variability analysis was verified with the Mauchly's Test. If there is a breach of the agreement, the Greenhouse-Geisser solution or the results of the analysis with MANOVA without this pre-agreement can be used.

The effects of abutment connection, position, and surface differences (4 × 2 × 4) were analyzed using three-way repeated ANOVA variability analysis, with the surface as a body factor in the sample unit (within-subject factor). The differences between groups and positions were determined by pairwise comparisons and controlled by the Bonferroni method. The tests were performed at a significance level of 0.05.

RESULTS

As shown in Table 2 and Figure 7, comparing the mean of the microstrain around two non-parallel implant-supported prostheses, group 2 (non-engaging, non-engaging) showed the highest compressive microstrains (-52.975), followed by control group 1 (engaging, angled abutment) (-25.239). Group 3 (SCRP-
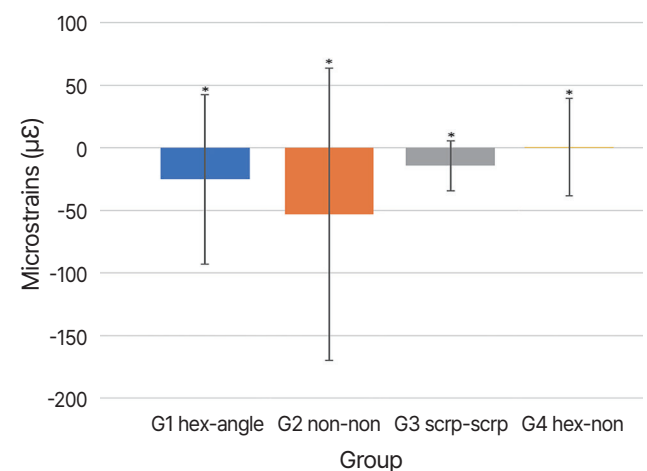

Fig. 7. Bar chart representing means and standard deviations of microstrains of each tested group, and * indicates the mean difference is significant at the 0.05 level.

Table 2. The mean values and standard deviations of the microstrain around two non-parallel implant-supported prostheses in the posterior region in four groups

Microstrains Group	N (Repeated)	Mean microstrains	Standard deviation
G1 control (hex, angle abutment)	10	-25.239*	67.737
G2 non-hex, non-hex	10	-52.975*	116.745
G3 scrp, scrp	10	-14.505*	19.911
G4 hex, non-hex	10	+0.418*	39.017

* Indicated the mean difference is significant at the 0.05 level, - = compression, + = tensile, hex = engaging, non-hex = non-engaging

SCRP) had the lowest compressive microstrains (-14.505), while only group 4 (engaging, non-engaging abutment) had tensile microstrains (0.418). Microstrains in groups 3 and 4 were significantly lower than those in the control group (*p*-value < .05).

As demonstrated in Table 3 and Figure 8, comparing the mean of the microstrain around two non-parallel implant-supported prostheses in two positions, area 45 showed compressive microstrains (-47.06) and area 47 had tensile microstrains (+0.91). Microstrains in area 45 were significantly higher than in area 47 (*p*-value < .05).

Comparing the mean of the microstrain around two non-parallel implant-supported prostheses on each surface in all groups, the highest compressive microstrains were recorded on the mesial surface of implant 45 in group 2 (non-engaging-non-engaging) (-333.87), and the highest tensile microstrains were recorded on the buccal surface of implant 45 in group 4 (engaging-non-engaging) (+51.07) and on the lingual surface of implant 45 in the control group (engaging-angled abutment) (+50.75) (Table 4, Fig. 9, and Fig. 10).

Table 3. The mean values and standard deviations of the microstrain around two non-parallel implant-supported prostheses in the posterior region in 2 positions

Microstrains Position	N (Repeated)	Mean microstrains	Standard deviation
45	10	-47.06*	94.13
47	10	+0.91*	27.45

* Indicated the mean difference is significant at the 0.05 level.

DISCUSSION

One of the indicators of the long-term success of implant-supported prostheses is the strain around dental implants and surrounding bone.[16,17] Abutment screw fracture, porcelain chipping, peri-implant bone loss, dental implant fracture, and loss of osseointegration are all possible outcomes of strains beyond the threshold values. In this study, microstrain was evaluated in two non-parallel implant-supported prostheses in the posterior region with various abutment connections and positions. The abutment connection and position of the abutments demonstrated

Fig. 8. Bar chart representing means and standard deviations of microstrains around two non-parallel implant-supported prostheses in each position, and * indicates the mean difference is significant at the 0.05 level.

Table 4. The mean values and standard deviations of the microstrain around two non-parallel implant-supported prostheses in the posterior region on each surface in all groups

Group	N	Mesial 45	Distal 45	Buccal 45	Lingual 45	Mesial 47	Distal 47	Buccal 47	Lingual 47
1	10	-146.30 (5.89)	+38.50 (5.45)	-97.46 (8.34)	+50.75 (8.47)	+47.63 (7.36)	-29.11 (6.07)	-51.28 (9.40)	-14.64 (9.38)
2	10	-333.87 (5.24)	+18.64 (3.92)	-121.42 (5.52)	+28.20 (6.45)	-36.01 (3.15)	+13.46 (2.87)	-19.03 (5.58)	+26.24 (10.32)
3	10	-37.70 (2.85)	-25.34 (3.43)	-38.43 (3.64)	-18.62 (3.67)	+6.35 (3.54)	+2.72 (4.77)	-21.93 (4.64)	+16.92 (4.78)
4	10	-16.18 (1.51)	-78.91 (3.25)	+51.07 (2.59)	-25.89 (2.27)	+7.85 (2.96)	+35.97 (2.66)	+0.46 (3.30)	+28.96 (4.59)

*1 = hex-angled, 2 = non-non, 3 = SCRP-SCRP, 4 = hex-non

Fig. 9. Bar chart representing means and standard deviations of microstrains around two non-parallel implant-supported bridges of each surface at implant 45.

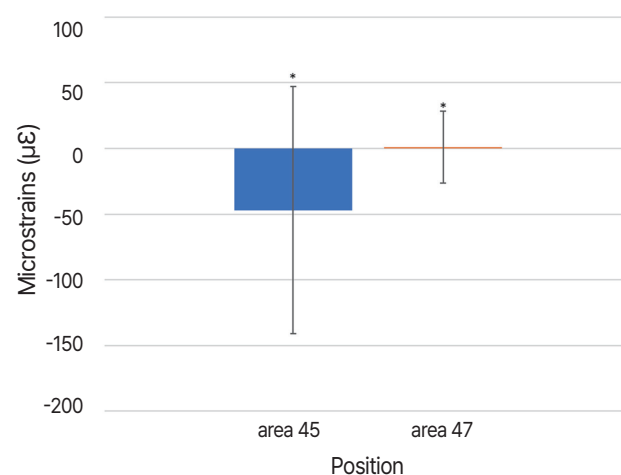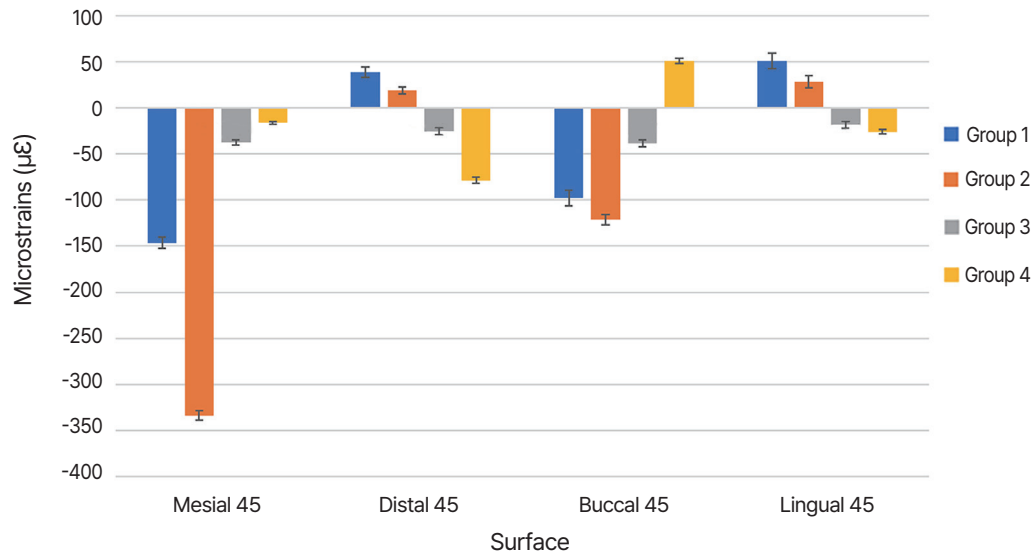**Fig. 10.** Bar chart representing means and standard deviations of microstrains around two non-parallel implant-supported bridges of each surface at implant 47.
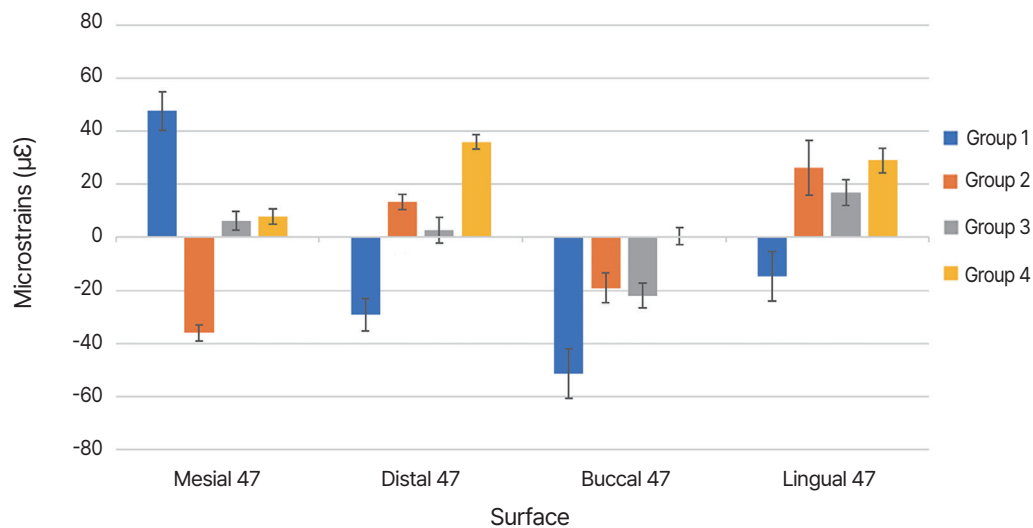
a potential effect on microstrain at the implant-bone interface of two non-parallel implant-supported prostheses in the posterior region. The null hypothesis was rejected, i.e., the type and position of the abutments showed significant differences in microstrain values at the implant-bone interface of two non-parallel implant-supported prostheses in the posterior region.

In this study, both non-engaging abutments had the most microstrains on the bone. Both SCRP abutments had the least microstrains on the bone. Therefore, if two implants are not parallel, SCRP-SCRP abutments could be possible options. Because SCRP abutments have both engaging and non-engaging parts, they offer passive fit, retrievability, and space compensation for nonparallel implants when two implants make an angle of no more than 20 degrees, with advantages in

screw- and cement-retained prostheses for extraoral or intraoral cases.[9] Moreover, the result of this study showed that SCRP abutments gave the lowest compressive microstrains on the bone. Group 2 (non-engaging, non-engaging) had the highest microstrains around two non-parallel implant-supported prostheses. Although the non-engaging abutment has a larger implant-abutment tight contact area, when the engaging abutment is loaded, the position of the contact area is likely to become deeper than the non-engaging abutment, which enlarges this area at the implant-abutment interface and reduces the strain and stress on the abutment screw. This decreases micromovement, offering the advantage of having better fit between implant components.[18] The results were similar to those of Savignano et al.,[6] which used FEA to study the stress distribution on mandibular screw-retained FDP when using different combinations of engaging and non-engaging abutments. They found that the cancellous and cortical bones in both non-engaging abutments had the highest stress. If all implants are parallel in the restoration and have a passive fit, both engaging abutments are recommended because they have the optimum stress distribution. On the other hand, if implants are not parallel, the alternative is to utilize a combination of an engaging abutment and a non-engaging abutment. The outcomes of the current experiment were also in line with those of Dogus et al.,[10] who looked at the fatigue response of the effects of internally connected engaging component position in screw-retained fixed cantilevered prostheses and found that both non-engaging components had a lower cycle number before fracture and a lower axial force at fracture, meaning that a screw-retained cantilevered FDP with an engaging abutment has a mechanical advantage in that it requires less force and fewer cycles to fail early. However, both implants must be parallel; if they are not, it is would better to use an engaging abutment in the implant that is farthest from the cantilever to increase resistance to abutment screw fracture. The SCRP abutment has less contact area between the implant and the SCRP abutment than with the engaging abutment. However, Linkevicius[1] discovered that engaging and non-engaging abutments have the same conical connection that allows them to engage the implant. A contact plane exists between the implant and abutment, known as a conical connection. The hex in the implant and the engaging abutment are not physically touching. Therefore, since loads are delivered to the implant with a conical connection, load transfer is the same for engaging and non-engaging abutments. Future direct comparisons, in potential clinical trials, would be of high value in order to explore which type offers the best resistance to microstrains, with the least change of technical complications.

In the present study, group 4 (engaging, non-engaging) had the lowest microstrain and tensile microstrain. It is important to keep in mind that dental implants and bone prefer compressive stress over tensile stress, since the implant-bone interface is typically maintained by compressive loads. This contact is typically disturbed by tensile and shear forces. Shear force might damage the implant and the bone.[19] From this study, it was found that different abutment connections had a possible influence on stress distribution. There is less contact area between the implant and the SCRP abutment than with the engaging abutment; however, the microstrain value is lower than in the control group. This may be due to other factors, such as the position of the strain gauge and the load distribution on the crown in each model. Based on the outcomes of this study, it is proposed to use both SCRP abutments in two non-parallel implant-supported prostheses when two implants make an angle no more than 20 degrees, followed by a combination of engaging and non-engaging as another option. Further experiments and future clinical comparisons are necessary to determine its accuracy.

Additionally, using a combination of engaging and non-engaging abutments, or both non-engaging abutments, can also be implemented to leave a specific amount of space between the dental implants and provide a passive fit. According to a related study by Rutkunas et al.,[20] which assessed the fit of a two-implant-supported screw-retained zirconia framework with three different combinations of abutment connections (both engaging, engaging and non-engaging, and both non-engaging), it was discovered that both non-engaging two-implant-supported zirconia frameworks tolerated the vertical and hori-

zontal misfit levels better. Because both engagement frameworks are more susceptible to minute distortions that can happen throughout the prosthetic procedure, they are less advised for 2-implant-supported FDPs. The prosthesis and peri-implant bone are under more stress with higher levels of misfit.[21,22]

Based on the results of a study by Cavallaro and Greenstein,[23] an increased stress on implants is seen if angled abutments are used; nevertheless, these increases were within physiological limits. Consequently, it was anticipated that the angled abutment implant at area 47 in the control group should have more microstrains than the straight abutment implant at area 45. However, this study found that straight abutments had a larger microstrain. In other words, the microstrain of implant area 47 was lower in this study, even with implants that were 15° inclined and an angled abutment. This was likely due to the fact that the implant in area 45 was 4.0 mm in diameter, smaller than the implant in area 47, which was 5.0 mm in diameter. In addition, the implant in site 45 had an anterior and posterior cantilever. This agrees with Eazhil *et al*.[24] and Matsushita *et al*.,[25] who discovered that the use of implants with a smaller diameter led to an overall increase in the amount of stress and strain around the implant. This might be as a result of these implants' smaller size and surface area, which exert more force per square millimeter of enclosing bone than larger-diameter implants.[26] The result was also in line with the study by Lee *et al*.,[27] which revealed that implant diameter affects the stress distribution on the implant complex; as implant diameter decreases, stress concentration increases. A 1 mm increase in diameter results in a 15% reduction in stress. This study suggests that the diameter may have a greater impact on microstrain distribution than the implant's 15-degree angulation.

Microstrains surrounding the peri-implant bone at implant in area 45 in this study were higher than at implant 47 in all groups. In addition, implant in area 45 had a smaller diameter, with cantilevers on the front and back of the implant, as mentioned previously, as opposed to implant in area 47, which only had an anterior cantilever. According to numerous earlier studies, the stress concentration surrounding the implants increased as cantilever length increased.[8,28,29]

Therefore, a short cantilever length is advised since it is the primary means of lowering stress on the cortical bone.[29] The greatest stresses were observed at the ridge crest on the distal surface of the distal implant for all cantilever lengths, and as cantilever lengths increased, the maximal stress on the implants also increased. According to studies by Suya Moura Mendes Alencar *et al*.,[30] it was shown that the effects of cantilever length on load transfer to the mandible distal cantilevers cause more stress to be distributed more unevenly throughout the peri-implant bone than mesial cantilevers. Therefore, if it is not possible to place one implant for each lost tooth, the use of cantilevers should be avoided because it increases the possibility of treatment failure.[31]

When the microstrain distribution on the FDP component is higher than the yield strength of the material, plastic deformation of the component can occur, leading to screw loosening. Additionally, high stress concentrations can lead to deformation and wear between components.[6] According to Frost,[32] bone responses to tension can be divided into four windows: acute disuse, adaptation, mild overload, and pathologic overload. The acute disuse window has tensions below 50 microstrains, resulting in bone loss. The adaptation window has tensions between 50 microstrains and 1,500 microstrains, resulting in a balance between resorption and formation. The mild overload window has tensions between 1,500 and 4,000 microstrains, resulting in an increase in the modeling process. The pathologic overload window has tensions above 4,000 microstrains, which indicate bone resorption. However, in this study, all groups had compressive and tensile microstrains within the physiological zone (1000 – 3000 microstrain). Because this study used bilateral static axial loading of 300 N, which is the average functional occlusal force, the load was transferred simultaneously and evenly to the crown and bridge, abutment connection, implant, and bone. It may make the microstrain value less than the physiological zone.

This study was modeled as an implant-supported prosthesis with 4-units in the posterior teeth, as it is the most common area for missing teeth. In general, most of the implant treatments are a single unit or bridge of three units. However, in this study, it was

modeled as a 4-unit implant-supported prosthesis. The reason is that a strain gauge can be attached around implants 45 and 47 to study the microstrains on the bone around the implant. A control group is used as an engaging and angled abutment and designed as a cement-retained implant-supported bridge because it is an option available to overcome when two implants are more non-parallel. It corrects the angle of the implant that is inclined to straighten the abutment and allows a bridge for easy insertion and passivity.

The results of this study must be interpreted in light of its limitations. As only models were used, this does not simulate nor reflect all clinical situations and oral environments. Moreover, the model used was a simulated trabecular bone, which has Young's modulus of 2.2 GPa. However, in reality, bones may have different densities in a certain location. The actual strain value in human bone in the area in contact with the implant surface could also potentially be higher, compared to this *in vitro* study, since the strain gauge was attached 2 mm away from the implant surface. Additionally, two non-parallel implant-supported prostheses of four units were studied, applying only vertical static load, and one implant brand was chosen. Therefore, the analyzed aspects should be investigated in further experiments and clinical studies with various numbers of units, as well as different implant sizes and manufacturers, evaluating both static and cyclic loads in the occlusal oblique direction, in order to provide greater clarity on the factors causing implant complications and failures by extending it to different designs and components.

It is also recommended to use finite element analysis in future investigations, which can assess microstrain distribution on various implant designs, abutment screws, and bones, in order to potentially reach useful guidelines for implant components selection in a clinical setting.

CONCLUSION

Within the limitations of this *in vitro* study, different abutment types (engaging, angled abutment, non-engaging, and SCRP) and different abutment position types (areas 45 and 47) had different microstrain effects on the bone around the implant. Both SCRP abutments could be a possible option to utilize in non-parallel implant-supported prostheses when two implants make an angle of no more than 20 degrees. If an angle greater than 20 degrees is present between the 2 implants, a combination of engaging and non-engaging abutments might be alternatives to use in non-parallel implant-supported prostheses.

REFERENCES

1. Linkevicius T. Zero bone loss concepts. 1st ed. Quintessence Publishing Company, Incorporated, llinois, USA; 2019. p. 181-93.

2. Wittneben JG, Joda T, Weber HP, Brägger U. Screw retained vs. cement retained implant-supported fixed dental prosthesis. Periodontol 2000 2017;73:141-51.

3. Ma S, Fenton A. Screw- versus cement-retained implant prostheses: a systematic review of prosthodontic maintenance and complications. Int J Prosthodont 2015;28:127-45.

4. Quaresma SE, Cury PR, Sendyk WR, Sendyk C. A finite element analysis of two different dental implants: stress distribution in the prosthesis, abutment, implant, and supporting bone. J Oral Implantol 2008;34:1-6.

5. Jafarian M, Mirhashemi FS, Emadi N. Finite element analysis of stress distribution around a dental implant with different amounts of bone loss: an in vitro study. Dent Med Probl 2019;56:27-32.

6. Savignano R, Soltanzadeh P, Suprono MS. Computational biomechanical analysis of engaging and non-engaging abutments for implant screw-retained fixed dental prostheses. J Prosthodont 2021;30:604-9.

7. Schnutenhaus S, Wagner M, Edelmann C, Luthardt RG, Rudolph H. Factors influencing the accuracy of freehand implant placement: a prospective clinical study. Dent J (Basel) 2021;9:54.

8. Suedam V, Moretti Neto RT, Sousa EA, Rubo JH. Effect of cantilever length and alloy framework on the stress distribution in peri-implant area of cantilevered implant-supported fixed partial dentures. J Appl Oral Sci 2016;24:114-20.

9. Heo YK, Lim YJ. A newly designed screw- and cement-retained prosthesis and its abutments. Int J Prosthodont 2015;28:612-4.

10. Dogus SM, Kurtz KS, Watanabe I, Griggs JA. Effect of engaging abutment position in implant-borne, screw-retained three-unit fixed cantilevered prostheses. J Prosthodont 2011;20:348-54.

11. Silveira MPM, Campaner LM, Bottino MA, Nishioka RS, Borges ALS, Tribst JPM. Influence of the dental implant number and load direction on stress distribution in a 3-unit implant-supported fixed dental prosthesis. Dent Med Probl 2021;58:69-74.

12. Sallam H, Kheiralla LS, Aldawakly A. Microstrains around standard and mini implants supporting different bridge designs. J Oral Implantol 2012;38:221-9.

13. Dos Santos Marsico V, Lehmann RB, de Assis Claro CA, Amaral M, Vitti RP, Neves ACC, da Silva Concilio LR. Three-dimensional finite element analysis of occlusal splint and implant connection on stress distribution in implant-supported fixed dental prosthesis and peri-implantal bone. Mater Sci Eng C Mater Biol Appl 2017;80:141-8.

14. Rungsiyakull P, Kujarearntaworn K, Khongkhunthian P, Swain M, Rungsiyakull C. Effect of the location of dental mini-implants on strain distribution under mandibular Kennedy Class I implant-retained removable partial dentures. Int J Dent 2021;2021:6688521.

15. Kim HY. Statistical notes for clinical researchers: assessing normal distribution (2) using skewness and kurtosis. Restor Dent Endod 2013;38:52-4.

16. Schwarz MS. Mechanical complications of dental implants. Clin Oral Implants Res 2000;11:156-8.

17. Liaw K, Delfini RH, Abrahams JJ. Dental Implant Complications. Semin Ultrasound CT MR 2015;36:427-33.

18. Lee H, Park SM, Noh K, Ahn SJ, Shin S, Noh G. Biomechanical stability of internal bone-level implant: Dependency on hex or non-hex structure. Struct Eng Mech 2020;74:567-76.

19. Amini AR, Laurencin CT, Nukavarapu SP. Bone tissue engineering: recent advances and challenges. Crit Rev Biomed Eng 2012;40:363-408.

20. Rutkunas V, Dirse J, Kules D, Simonaitis T. Misfit simulation on implant prostheses with different combinations of engaging and nonengaging titanium bases. Part 1: Stereomicroscopic assessment of the active and passive fit. J Prosthet Dent 2023;129:589-96.

21. Janda M, Larsson C, Mattheos N. Influence of misfit on the occurrence of porcelain veneer fractures in implant-supported metal-ceramic fixed dental prosthe-

ses. Part 2: a three-dimensional finite element analysis. Int J Prosthodont 2021;34:458-62.

22. Toia M, Stocchero M, Jinno Y, Wennerberg A, Becktor JP, Jimbo R, Halldin A. Effect of misfit at implant-level framework and supporting bone on internal connection implants: mechanical and finite element analysis. Int J Oral Maxillofac Implants 2019;34:320-8.

23. Cavallaro J Jr, Greenstein G. Angled implant abutments: a practical application of available knowledge. J Am Dent Assoc 2011;142:150-8.

24. Eazhil R, Swaminathan SV, Gunaseelan M, Kannan GV, Alagesan C. Impact of implant diameter and length on stress distribution in osseointegrated implants: A 3D FEA study. J Int Soc Prev Community Dent 2016;6:590-6.

25. Matsushita Y, Kitoh M, Mizuta K, Ikeda H, Suetsugu T. Two-dimensional FEM analysis of hydroxyapatite implants: diameter effects on stress distribution. J Oral Implantol 1990;16:6-11.

26. Flanagan D. Fixed partial dentures and crowns supported by very small diameter dental implants in compromised sites. Implant Dent 2008;17:182-91.

27. Lee H, Jo M, Sailer I, Noh G. Effects of implant diameter, implant-abutment connection type, and bone density on the biomechanical stability of implant components and bone: A finite element analysis study. J Prosthet Dent 2022;128:716-28.

28. Rubo JH, Capello Souza EA. Finite-element analysis of stress on dental implant prosthesis. Clin Implant Dent Relat Res 2010;12:105-13.

29. Oyar P, Durkan R, Deste G. The effect of the design of a mandibular implant-supported zirconia prosthesis on stress distribution. J Prosthet Dent 2021;125:502.e1-11.

30. Alencar SM, Nogueira LB, Leal de Moura W, Rubo JH, Saymo de Oliveira Silva T, Martins GA, Moura CD. FEA of peri-implant stresses in fixed partial denture prostheses with cantilevers. J Prosthodont 2017;26:150-5.

31. de Souza Batista VE, Verri FR, Almeida DA, Santiago Junior JF, Lemos CA, Pellizzer EP. Finite element analysis of implant-supported prosthesis with pontic and cantilever in the posterior maxilla. Comput Methods Biomech Biomed Engin 2017;20:663-70.

32. Frost HM. A 2003 update of bone physiology and Wolff's Law for clinicians. Angle Orthod 2004;74:3-15.